Available online at www.sciencedirect.com
ScienceDirect
Estuarine, Coastal and Shelf Science 71 (2007) 523–536
ESTUARINE COASTAL AND SHELF SCIENCE
www.elsevier.com/locate/ecss

An inflection in the rate of early mid-Holocene eustatic sea-level rise: A new sea-level curve from Singapore

M.I. Bird [a,*], L.K. Fifield [b], T.S. Teh [c], C.H. Chang [c], N. Shirlaw [d], K. Lambeck [e]

[a] School of Geography and Geosciences, University of St. Andrews, Irvine Building, St. Andrews, Fife, KY16 9AJ Scotland, UK
[b] Research School of Physical Sciences and Engineering, Australian National University, Canberra, A.C.T. 0200, Australia
[c] National Institute of Education, Nanyang Technological University, 1 Nanyang Walk, Singapore 637616, Singapore
[d] Land Transport Authority, 1 Hampshire Road, Singapore 219428, Singapore
[e] Research School of Earth Sciences, Australian National University, Canberra, A.C.T. 0200, Australia

Received 3 July 2006; accepted 4 July 2006
Available online 13 December 2006

Abstract

This study presents a sea-level curve from ~9500 to ~6500 cal BP for the farfield location of Singapore, on the Sunda Shelf in southeast Asia. The curve is based on more than 50 radiocarbon dates from elevations of +1.43 m to −15.09 m representing sea-level index points in intertidal mangrove and shallow marine sediments deposited by sea-level rise accompanying deglaciation. The results indicate that mean sea level rose rapidly from around −17 m at 9500 cal BP to around −3 m by 8000 cal BP. After this time, the data suggest (but do not unequivocally prove) that the rate of sea-rise slowed for a period of 300–500 years centred on ~7700 cal BP, shortly after the cessation of meltwater input to the oceans from the northern hemisphere. Renewed sea-level rise amounting to 3–5 m began around 7400 cal BP and was complete by 7000 cal BP. The existence of an inflection in the rate of sea-level rise, with a slow-down centred on ~7700 cal BP, is broadly consistent with other available sea-level curves over this interval and is supported by evidence of stable shorelines and delta initiation elsewhere at this time, as well as evidence of comparatively rapid retreat of the West Antarctic ice sheet beginning around 7500 cal BP. 'Stepped' sea-level rise occurring shortly after 7500 cal BP and also earlier during deglaciation may have served to focus significant post-glacial episodes of human maritime/coastal dispersal, into comparatively narrow time intervals.

Keywords: Holocene; sea level; radiocarbon; Sundaland; mangrove; palaeoclimate

1. Introduction

Melting of the extensive high latitude/altitude icecaps of the Last Glacial Maximum led to an increase in global eustatic sea-level of ~120 m (Clark and Mix, 2002; Lambeck et al., 2002a,b). Fairbanks (1989) first demonstrated that the rate of meltwater input during deglaciation was not constant, identifying two meltwater pulses (MWP-1A, ~14,000 cal BP; MWP-1B, 11,000 cal BP) from the dating of coral cores collected from Barbados. Additional data from Caribbean coral records was subsequently interpreted by Blanchon and Shaw (1995) as indicating a further, later and smaller meltwater pulse (MWP-2, ~7600 cal BP).

While the existence of MWP-1A has been generally confirmed by subsequent work (e.g. Okuno and Nakada, 1999; Hanebuth et al., 2000) the existence, timing and magnitude of other possible episodes of stepped sea-level rise continue to be debated (Bard et al., 1996; Okuno and Nakada, 1999; Shennan, 1999; Blanchon et al., 2002; Liu et al., 2004). Of postulated later meltwater pulses, MWP-2, as defined by Blanchon and Shaw (1995) is of particular significance. The notional timing of MWP-2 and the preceding 600–800 years encompasses the most significant climatic excursion of the Holocene (the 8.2 ka 'event'; Alley et al., 1997; Clark et al., 2001), associated

* Corresponding author.
E-mail address: michael.bird@st-andrews.ac.uk (M.I. Bird).

0272-7714/$ - see front matter © 2006 Elsevier Ltd. All rights reserved.
doi:10.1016/j.ecss.2006.07.004

with rapid but small increases in global sea-level associated with the draining of freshwater lakes dammed by the Laurentide ice-sheet (Clark et al., 2001). This period also encompasses the flooding of the Black Sea (Ryan et al., 1997; Ballard et al., 2000 – but see also Aksu et al., 2002), the initiation of a global phase of delta progradation (Stanley and Warne, 1994), and comparatively small changes in the rate of sea-level rise over this period may have had a major impact on the distribution and stability of resource-rich marginal marine environments and thereby on prehistoric coastal communities (Stanley and Warne, 1997). However, the magnitude of these changes are comparatively small and hence difficult to unequivocally identify in the geological record.

Here we present a new, high-resolution sea-level curve for Singapore, a farfield location on the Sunda Shelf in Southeast Asia. This record covers the early to mid-Holocene period, a time that is critical for deepening our understanding of the complex linkages between climate, sea-level rise and human development and dispersal. Although data was also collected on sea level in Singapore since the mid-Holocene, discussion in this paper is restricted to the critical interval of rapid deglacial sea-level rise prior to 6500 cal BP.

2. Study area and previous investigations

The island state of Singapore lies off the southern tip of the Malaysian Peninsula, at the core of the now largely submerged ice-age continent of Sundaland. During the Last Glacial Maximum the Sunda Shelf and the shallow seas between Peninsular Malaysia, Java, Sumatra and Borneo were fully exposed, becoming progressively flooded by post-glacial sea-level rise (Hanebuth et al., 2000). The region is remote from the areas of ice accumulation at the LGM, and is considered tectonically stable, although a recent analysis of the bathymetry of the Straits of Singapore and the Quaternary geology of Singapore has suggested the region has been undergoing slow downwarping at a rate of 0.06 to 0.1 mm/years since the beginning of the last Interglacial (Bird et al., in press).

Singapore is an ideal location for sea-level studies because most of the coastline is sheltered, wave fetch is generally short and tidal energy is low. Tides are currently semi-diurnal with mean spring tide range of 2.4 m and a mean neap tide range of 1 m (Wong, 1992). In addition, the longest river draining Singapore is <20 km long, meaning there is little opportunity for the storage and remobilization of sediment and woody debris that often confounds attempts to obtain reliable dates from larger deltas and other marginal marine environments (Stanley, 2001).

Previous sea-level studies in the region have indicated that post-glacial sea-level rise isolated the main island of Singapore from the Malaysian peninsula around the beginning of the Holocene (Hesp et al., 1998). The region is a 'farfield' location and hence sea-level rose above modern mean sea-level in the mid-Holocene producing a sea-level highstand variously determined to be 2–5 m above modern mean sea-level around Singapore and along the Malaysian coast to the north (Geyh et al., 1979; Tjia, 1992; Hesp et al., 1998). During this period of initial transgression and the subsequent sea-level highstand, thick sequences of marine and marginal marine sediments accumulated on the weathered pre-transgression land surface of Singapore. Subsequent gradual lowering of sea-level since the mid-Holocene has exposed the surface of these sediments over much of the area of modern Singapore below ~5 m above modern mean sea-level.

The nature of the sediments and basement lithologies underlying the Holocene transgressive sequence has been reviewed elsewhere (PWD, 1976; Pitts, 1983; Gupta et al., 1987; Bird et al., 2003) and is only relevant to this study insofar as their compressibility may impact upon the elevation of the sea-level index points discussed below. Three types of basement underlie the Holocene sediments sampled in this study: (1) weathered shales and sandstones of the early Jurassic Jurong Formation; (2) dense, highly consolidated (but not lithified) fluvial sands and clays of the Plio-Pleistocene 'Old Alluvium'; and (3) highly weathered and compacted (dry bulk density 1.5–1.9 g/cm^3; Bird et al., 2003) 'Lower Marine Clay', deposited during the earlier sea-level highstand of the Last Interglacial Period. Post Holocene-transgression and sediment loading is unlikely to have resulted in significant further compaction of any of these units.

The entire Holocene sedimentary cover of onshore Singapore is formally considered part of the genetically related Littoral (beach), Transitional (mangrove), Marine and Reef members of the Kallang and Tekong Formations (PWD, 1976). The earliest of these sediments associated with post-glacial sea-level rise were deposited as the highest tides associated with an approaching shoreline killed terrestrial vegetation. The resultant bare ground was exposed to severe erosion as a result of the locally intensely dissected land surface, easily erodable nature of the bedrock (the Old Alluvium in particular) and the high annual rainfall concentrated in short intense intervals. This led to the development of sandsheets with planar foresets intercalated with muddy sediments in the uppermost intertidal zone (Tekong Formation and parts of the Transitional member of the Kallang Formation), and similar deposits can be found accumulating in the upper intertidal zone today. The Tekong Formation represents the highest, and now partly exhumed, expression of this facies and hence can be considered genetically equivalent to sediments of the Transitional Member of the Kallang Formation (Bird et al., 2003).

As sea-level rose further, mangrove muds and peats of the Transitional member were deposited over the interbedded muds and sands. Thereafter, submergence below mean sea-level resulted in the deposition of a thin, winnowed, sandy/shelly interval of sediment followed by finely laminated shelly clays of the Marine Member of the Kallang Formation. Post mid-Holocene emergence of the Holocene transgressive sediments resulted in the seaward progradation of mangrove sediments of the Transitional Member, over sediments of the Marine Member. In some areas the marginal marine Transitional Member of the Kallang Formation are overlain in turn by peats deposited in a freshwater swamp forest environment. This model for interpreting the Holocene sedimentary cover of onshore Singapore is used as the basis for the development of the sea-level index points discussed in the next section.

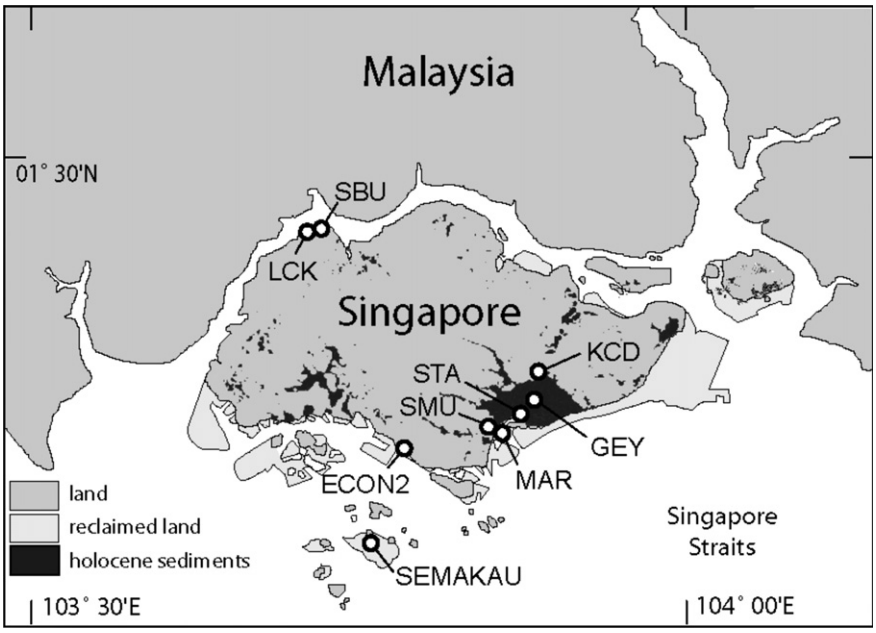

Fig. 1. Location map of Singapore showing sample locations used in this study. See Table 1for further information and explanation of prefixes. Note: ECON2 refers to the core location and SEMAKAU refers to coral locations of Hesp et al. (1998) as discussed in the text.

3. Experimental methods

3.1. Sampling

The sample sites chosen for this study are either vegetated mangrove swamps or construction sites where excavation exposed both the Holocene transgressive sediments and the underlying pre-transgression land surface. Over 1000 individual sediment samples were collected between 2001 and 2003 from multiple locations around Singapore (Fig. 1).

Sample locations were determined in the field using differential GPS to a horizontal accuracy of ±0.5 m, using the differential GPS signal broadcast from Raffles lighthouse, south of the main island of Singapore. Elevation was determined with reference to temporary benchmarks established by surveyors on individual construction sites that were in turn referenced to national benchmarks surveyed and maintained by the Singapore Land Authority (SLA). The elevation of mangrove sites was determined by levelling to an established SLA benchmark never more than 1 km distant. All sample elevations are accurate to ±0.05 m, and are reported relative to the land survey datum (mean sea level = 0 m) defined by the SLA, which is 1.652 m above the Chart datum used by the Admiralty on navigation charts for Singapore. The detailed locations of the sites sampled for this study are provided in Table 1.

Sediment cores were obtained using a 50 mm diameter modified Livingstone piston corer. The sediments were extracted in 1-metre increments with each section extruded on site and wrapped in plastic to prevent water loss prior to shipment to the laboratory. One deeper sediment core (GEY) was obtained by commercial contractor using a tractor-mounted 100 mm diameter hydraulic piston corer. Where excavations exposed the Holocene sequence to the underlying pre-transgression land surface, standing sections were cleaned and known

Table 1
Location and total range in elevation (relative to mean sea level) of samples collected for this study. Single sample locations are reported to ±0.5 m but where several locations were sampled at a single site, the approximate centre of the area only is provided at lower precision. Prefixes refer to radiocarbon dated samples in Table 3. Total elevation range refers to the total range for all samples collected at a site, not only radiocarbon dated samples

Prefix	General location	Type	Latitude (°N)	Longitude (°E)	Total elevation range (m)
GAM	Kampong Gambut, Johor	Outcrop	1.378056	104.280278	−0.5
GEY	Geylang, Singapore	Core	1.313713	103.891772	−3.0 to −30.9
KCD	Kim Chuan Depot, Singapore	Excavation	1.34010	103.88674	+4.4 to −2.2
LCK	Lim Chu Kang, Singapore	Core	1.446737	103.709312	+0.5 to −2.1
MAR	Suntec City, Singapore	Excavation	1.29090	103.86109	−5.9 to −8.1
SBU	Sungei Buloh, Singapore	Core	1.445231	103.734365	−0.7 to −3.7
SMU	Singapore Management Univ.	Excavation	1.29530	103.85041	+0.8 to −6.4
SMU-BBP	Singapore Management Univ.	Core	1.29530	103.85041	+1.0 to −2.4
STA	National Stadium, Singapore	Excavation	1.303760	103.877580	−7.8 to −10.0

volumes sampled at 5 or 10 cm intervals by pushing a 36.5 mm diameter PVC tube horizontally into the sediment for 5 cm. The sample was sealed in a plastic bag for transport to the laboratory. Over 200 samples of macroscopic material, datable by radiocarbon (wood and shell) were separately collected from the exposures. All samples were stored frozen until further treatment.

3.2. Determination of sea-level index points

Holocene sea-level rise in Singapore deposited a relatively consistent and predictable sequence of sediments that can be readily related to position in the intertidal zone from the distribution of the same facies in the modern environment (Table 2). Bird et al. (2003, 2004a,b) have described the sedimentology and physical characteristics of exposed sections and cores representative of those that form the basis of this study, and hence detailed descriptions of individual sections are not presented here. Results typical of the sedimentary sequences sampled for this study are shown in Fig. 2. The following sea-level index points can be delineated based on their stratigraphic and sedimentologic characteristics.

3.2.1. Pre-transgression land surface

Regardless of underlying lithology, this can be readily identified by its high dry bulk density ($\sim >1.5$ g/cm^3) and low organic carbon content ($\sim 0.1\%$) with pronounced yellow, brown and red colours resulting from iron oxide accumulation within a generally bleached and highly weathered matrix.

3.2.2. Uppermost intertidal zone, highest astronomical tide (HAT) to mean high water spring (MHWS)

The initial sediments associated with the Holocene transgression, are generally organic poor sands containing occasional and isolated fragments of woody debris. These sediments range from a few tens of centimetres to about 2 m in thickness. Where of sufficient thickness, this unit commonly contains intercalated beds of dark reduced or partly oxidized clays and organic debris 1–5 cm in thickness. Dry bulk density is generally high (>1 g/cm^3) and organic carbon content is generally <0.5%.

Intercalated clay beds are only well preserved at locations where a significant thickness of impermeable mud was subsequently deposited over the location. In the higher elevation exposures of this basal unit, where the sediments were covered only by a thin layer of post mid-Holocene peats, the clays become wholly bleached, organic debris completely disappears and original bedding is progressively destroyed, ultimately forming a structureless white, stiff clayey sand. Samples obtained at the base of this unit are assumed to have been deposited upon, or soon after, the arrival of HAT at the location, while samples deposited within the unit are assumed to have been deposited between HAT and MHWS and the uncertainty associated with the elevation of MSL at the time of deposition calculated as difference in elevation between these two tidal ranges.

Table 2
Conversions to equivalent mean sea level and associated uncertainties assumed for sea-level index points discussed in the text, and applied to elevation data in Table 3 (HAT = highest astronomical tide; MHWS = mean high water spring; MSL = mean sea-level; MLW = mean low water)

Sea-level index point	Conversion to msl	Error +	Error −
HAT	−2.25	0.6	0.05
HAT to MHWS	−1.7	0.6	0.6
MHWS (to MSL)	−1.15	0.63	0.05
MHWS to MSL	−0.58	0.63	0.63
MSL	0	0.63	0.63
MSL or below	0	0.8	0.05
MLW or above	0.8	0.4	0.4

3.2.3. Upper intertidal zone, mean high water spring (MHWS) to mean sea level (MSL)

As sea-level continued to rise, more frequent inundation resulted in a generally sharp transition to reduced, organic-rich sediments associated with the establishment of mangroves at the location. These sediments are from a few tens of centimetres to >4 m in thickness and are highly variable, ranging from sandy to clay-rich with organic material ranging from finely disseminated organic fragments to tree trunks and branches. Mangroves in the modern environment in Singapore extend from approximately MHWS to MSL. A common feature of these sediments is a basal organic peat, generally a few tens of centimetres in thickness and characterized by low bulk density ($< \sim 0.5$ g/cm^3) and high organic carbon content (~ 20–40%). Samples obtained at the base of this unit are assumed to have been deposited upon, or soon after, the arrival of MHWS at the location, and MSL is calculated on this basis, with the elevation uncertainty quoted as half the elevation difference between MHWS and MSL. This basal peat is commonly overlain, across a comparatively sharp transition, by an organic- and clay-rich mangrove mud with a dry bulk density between 0.5 and 0.8 g/cm^3 and organic carbon content of 5–10%. Samples deposited within this unit are assumed to have been deposited approximately at MSL with the uncertainty in elevation quoted as half the difference in elevation between MSL and MHWS above and between MSL and mean low water (MLW) below.

At higher elevations, these mangrove sediments are overlain in turn by a regressive sequence of increasingly organic-rich peats (ultimately deposited in a freshwater swamp forest environment), while at lower elevations, they are overlain by shallow marine sediments deposited after continued transgression.

3.2.4. Lower intertidal and sub-tidal zone, mean sea level (MSL) and below

At locations at lower elevation (e.g. STA), where mangrove sediment accumulation rates could not keep pace with rising sea level, the mangrove sediments are overlain by shallow marine shelly clays, often with a narrow interval composed of shelly sands immediately above the mangrove sediments. Samples obtained at the base of this unit are assumed to have been deposited upon, or soon after, the arrival of MSL at the location, and the uncertainty associated with the

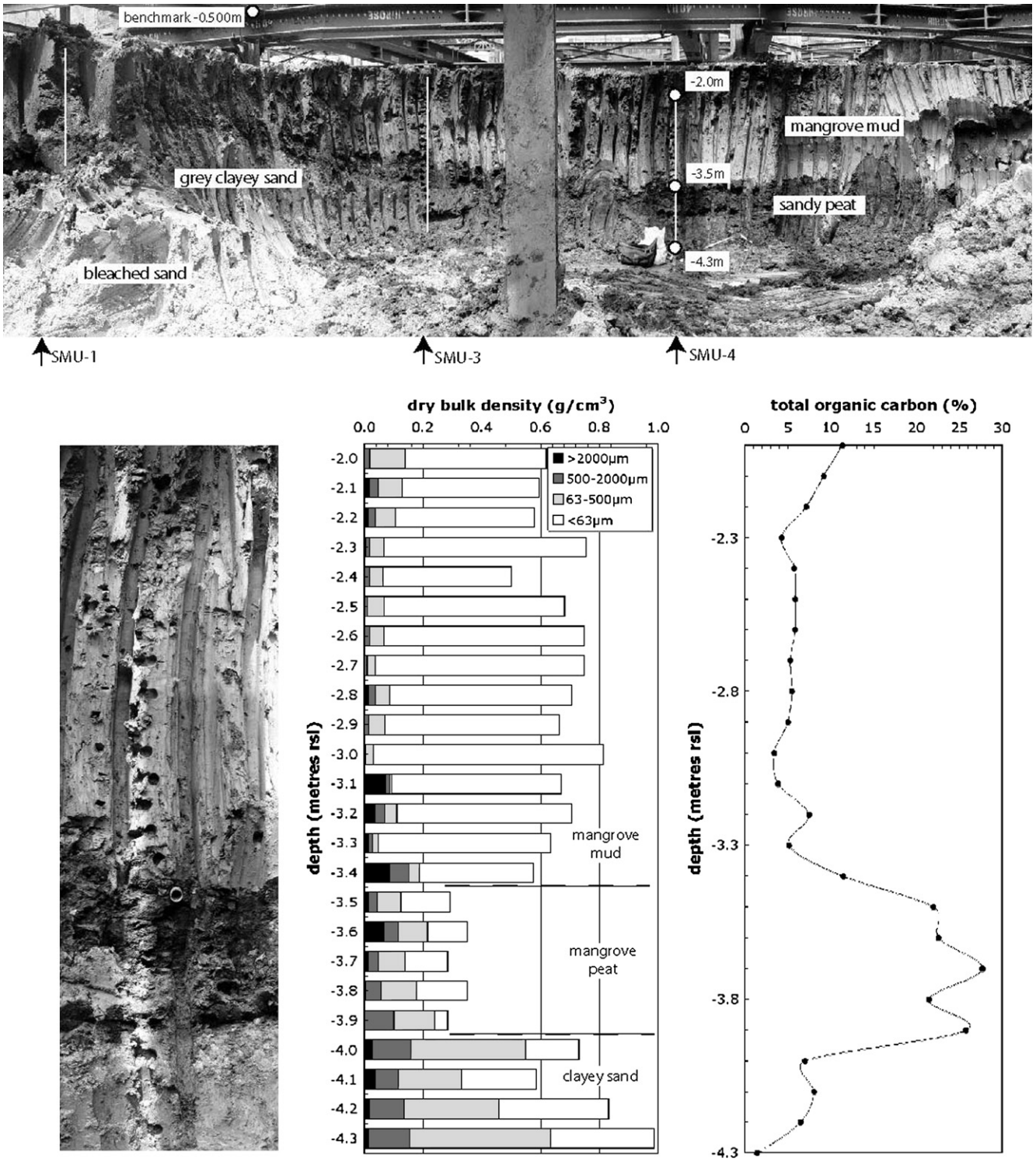

Fig. 2. Excavated face in Singapore Management University construction site, Bras Basah Road, Singapore. Upper panel shows the location of sections SMU-2, SMU-3 and SMU-4 and the general stratigraphy, from pre-transgression land surface, through mangrove peat to mangrove mud at the top of the section. A close-up of sequence at SMU-4 is shown in the left panel, with bulk density and particle size distribution data provided in the centre panel and organic carbon content in the right panel.

elevation of MSL at the time of deposition calculated on the assumption that the samples were deposited between MSL and MLW. Samples obtained from within the shallow marine 'Marine Clay', which may be up to 20 m in thickness can only be said to have been deposited below MSL. Such samples do not provide sufficient constraint on the elevation of MSL and hence are not included in the sea-level reconstruction. Molluscs from within the Upper Marine Clay, dated by Hesp et al. (1998) fall into this category and these dates are not considered in this study.

3.2.5. Sub-tidal zone, mean low water (MLW) and below

While most samples in this study are derived from mangrove sequences, radiocarbon dates on large (>1 m diameter) coral heads presented by Hesp et al. (1998) from Singapore and a single coral collected for this study in nearby Johor (Malaysia) can provide significant additional constraints on sea-level in the region. Observations by Hilton and Ming (1999) and levelling conducted for this study suggest that small coral heads currently grow up to about mean low water neap (MWLN) tide levels on reef flats around Singapore. We assume that the large coral heads dated for this study grew at mean low water (MLW) or below, with the uncertainty on this constraint on minimum MSL provided by the difference between MLWN and mean low water spring (MLWS) tides.

3.2.6. Representation of transgressive facies

It should be noted that not all facies are represented to the same degree in all sequences sampled for this study. For example, the intercalated sand/clay sediments assumed to relate to the uppermost intertidal zone between HAT and MHWS are most well developed at the Kim Chuan Depot (KCD) excavation site, where the Holocene transgressive sediments fill a steep-walled paleochannel incised into Old Alluvium. Rapid erosion of the Old Alluvium in this area provided an abundant supply of coarse clastic material which meant that this unit could 'keep pace' with rising sea-level and maintain the area in the uppermost intertidal zone for a comparatively long period before being transgressed by mangrove muds deposited between MHWS and MSL. The mangrove sediments also accumulated rapidly, so that marine clays were never deposited at the site as the mangroves could 'keep pace' with rising sea-level at this location. Conversely, the sediments immediately overlying the pre-transgression land surface in a hydraulic piston core from the Geylang area (GEY) are shelly clay-sands followed by marine clay. This stratigraphy likely resulted from there being no source of abundant sand available from erosion of the underlying Lower Marine Clay coupled with a rate of sea-level rise that was too fast to allow the deposition of any intertidal sediment, or, if intertidal sediments were deposited, these sediments were subsequently eroded by the advancing sea.

3.2.7. Autocompaction correction

Post-depositional compaction of sediments can significantly lower the elevation of a sample collected from within a sedimentary sequence, particularly when the underlying sediments are fine-grained and/or organic-rich (e.g. Allen, 2000). Where samples were collected from within a sedimentary sequence rather than at the contact with the pre-transgression land surface and where the sedimentary sequence is fine-grained and/or organic-rich, a correction for post-depositional compaction was applied using the methodology described by Bird et al. (2004b), involving a comparison of the dry bulk density, organic content and grain-size distribution of a compacted sample with the uncompacted dry bulk density of a modern sediment sample with the same organic matter and grain-size characteristics. Intervals where the sediments were dominated by organic-poor sand were considered to have undergone negligible post-depositional compaction.

For all but one sample, the compaction correction amounted to less than 0.6 m (and mostly less that 0.2 m) with the error on elevation associated with the correction being given by the difference between the elevation as measured in the field and the maximum calculated correction for autocompaction. This error was added in quadrature to the errors associated with surveying and the determination of the MSL indicated by the sample.

3.3. Radiocarbon dating and calibration

Samples were hand-picked and visually inspected for contamination before being washed thoroughly in demineralized water and dried prior to submission for dating. Organic samples were subjected to standard acid-base-acid pre-treatment to remove contamination. Samples were dated by conventional scintillation counting at the Research School of Earth Sciences, Australian National University (ANU-prefix) and by accelerator mass spectrometry both at the Research School of Physical Sciences and engineering, Australian National University (ANUA-prefix) and the Scottish Universities Environmental Research Centre (GU-prefix). Conventional radiocarbon dates (years BP) were converted to calendar dates (cal BP) using the Intcal98 dataset of Stuiver et al. (1998) and OxCal version 3.9 (Bronk Ramsey, 2001).

Carbonates formed in marine environments are also subject to a marine reservoir effect and this applies to the marine carbonate samples dated both in this study and by Hesp et al. (1998). Southon et al. (2002) reports a ΔR value of -122 ± 60 years for Singapore based on the analysis of a single bivalve collected from Singapore in 1860. However, the average ΔR value for the south/central South China Sea is -25 ± 20 years ($n = 10$) and this value has been adopted here for the mid-Holocene coral samples ($\sim$6000–7000 years BP), which all come from locations exposed to open ocean circulation. Dating of co-deposited wood and bivalves suggest that during the earlier Holocene, when sea-level was 5–15 m lower than the mid-Holocene, the local ΔR value was substantially larger (-386 ± 53 years), presumably the result of a restricted connection to the open ocean through the much narrower and shallower Singapore Straits coupled with the estuarine nature of the environment in which the molluscs were living. This value has been adopted for mollusc samples in this study ($\sim$7000–8000 years BP).

4. Results

A summary of sample locations and elevations is provided in Table 1, and individual sample elevations, calculated equivalent MSL, radiocarbon dating results and the data of Hesp et al. (1998) is provided in Table 3. Over 50 samples were dated for this study spanning elevations from +1.43 m to −15.09 m, and yielding ages ranging from 5890 to 8405 years BP. Fig. 3 indicates that the samples are approximately evenly distributed in elevation down to −8 m, with fewer samples

Table 3
Elevation, type and radiocarbon results for samples dated as part of this study. Also shown for each sample is sea level index point, decompaction correction and elevation of mean sea-level (MSL) inferred for the time of sample deposition, including the associated uncertainty. Laboratory prefixes are as described in the text. Radiocarbon dates are quoted in radiocarbon years with 1 s uncertainty and also as the calibrated 1s range of ages. Note: *samples used to calculate reservoir correction for early mid-Holocene carbonates; (1) ΔR of -25 ± 63 years applied (Southon et al., 2002); ΔR of -386 ± 53 years applied. Calibrated radiocarbon ages also shown for samples of Hesp et al. (1998)

Sample	Elevation (m)	Indicates	Material	Decompaction (m)	Inferred msl (m)	Error+ (m)	Error− (m)	Prefix	Lab No.	^{14}C age (years BP)/ error (years)	Lower (1σ) (cal BP)	Upper (1σ) (cal BP)
KCD-13 +15 cm	1.43	MHWS	Wood	0.16	0.36	0.61	0.09	ANU-	11810	6190 ± 70	7210	6990
KCD-6 +30 cm	1.33	MHWS	Wood	0	0.18	0.60	0.05	ANU-	11806	6300 ± 80	7320	7030
KCD-6 +25 cm	1.28	MHWS	Wood	0	0.13	0.60	0.05	ANUA-	26403	6506 ± 186	7590	7240
KCD-12 0 cm	1.27	HAT to MHWS	Wood	0	−0.43	0.60	0.60	ANU-	11809	6140 ± 90	7160	6890
SMU-BBP-2 204	0.70	MHWS to MSL	Wood	2.00	1.13	1.17	1.17	ANUA-	19525	6157 ± 156	7250	6800
KCD-4D 0 cm	0.70	MHWS	Wood	0	−0.45	0.60	0.05	ANU-	11802	6200 ± 90	7250	6990
KCD-4E −10 cm	0.60	MHWS	Wood	0	−0.55	0.60	0.05	ANU-	11803	6000 ± 60	6900	6740
KCD-1E	0.50	MHWS to MSL	Wood	0.18	0.02	0.61	0.61	ANU-	11801	5890 ± 110	6860	6550
KCD-13 −120 cm	0.08	HAT	Wood	0.07	−2.14	0.60	0.06	ANU-	11811	7070 ± 130	8010	7740
KCD-13 −125 cm	0.03	HAT	Wood	0	−2.22	0.60	0.05	ANU-	11812	6650 ± 80	7580	7430
GAM coral 2a	−0.51	MLW or below	Coral (1)	0	0.29	0.4	0.4	ANU-	12000	6380 ± 90	7010	6730
SMU-11 +20 cm	−0.80	HAT	Wood	0	−3.05	0.60	0.05	ANU-	11994	7380 ± 100	8330	8040
SBU-1 1−3	−0.90	MHWS to MSL	Wood	0.75	−1.10	0.71	0.71	ANUA-	22729	6398 ± 190	7600	7000
SMU-BBP140302	−0.94	MHWS	Wood	0	−2.09	0.60	0.05	ANUA-	22228	6704 ± 205	7790	7370
KCD-1B	−1.10	MHWS	Wood	0	−2.25	0.60	0.05	ANU-	11800	6750 ± 80	7680	7510
BBP-2 407 cm	−1.32	MHWS to MSL	Wood	0.06	−1.87	0.60	0.60	ANUA-	19526	6245 ± 147	7320	6940
SBU-1 1−7	−1.33	MHWS to MSL	Wood	0.55	−1.63	0.66	0.66	ANUA-	22728	6348 ± 190	7430	7010
SMU-BBP-2 430	−1.55	MHWS	Wood	0	−2.70	0.60	0.05	ANUA-	19527	6657 ± 166	7680	7370
SBU-1 2-1	−1.68	MHWS to MSL	Wood	0.4	−2.06	0.63	0.63	ANUA-	22727	6816 ± 200	7920	7480
KCD-14 +35 cm	−1.81	HAT	Wood	0	−4.06	0.60	0.05	ANU-	12048	7000 ± 80	7940	7740
KCD 14 +20 cm	−1.96	HAT	Wood	0	−4.21	0.60	0.05	ANU-	11799	7340 ± 70	8280	8030
SMU-2A	−2.00	MHWS	Wood	0	−3.15	0.60	0.05	ANU-	11988	6650 ± 110	7610	7430
LCK-4-3 4 cm	−2.04	MHWS	Wood	0	−3.19	0.60	0.05	ANUA-	22223	7092 ± 193	8110	7690
SMU-2B	−2.15	MHWS	Wood	0	−3.30	0.60	0.05	ANU-	11982	7150 ± 90	8110	7840
SBU 1-2-8	−2.48	MHWS	Wood	0	−3.63	0.60	0.05	ANUA-	22726	6820 ± 188	7850	7480
SMU-3 +80 cm A	−2.50	MSL	Wood	0.1	−2.45	0.60	0.60	ANU-	11985	6360 ± 240	7600	6950
SMU-3 +80 cm B	−2.50	MSL	Wood	0.1	−2.45	0.60	0.60	ANU-	11987	7160 ± 320	8350	7650
SMU-1 0 cm A	−2.60	MHWS	Wood	0	−3.75	0.60	0.05	ANU-	11989	7470 ± 160	8410	8050
SMU-1 0 cm B	−2.60	MHWS	Wood	0	−3.75	0.60	0.05	ANUA-	26328	6746 ± 187	7750	7430
SMU-3 +40 cm	−2.90	MSL	Wood	0.08	−2.86	0.60	0.60	ANU-	11983	7070 ± 90	7970	7790
SMU-4 0 cm	−3.50	MSL	Wood	0.08	−3.46	0.60	0.60	ANU-	11981	6500 ± 270	7700	7000
SMU-4 10 cm	−3.60	MSL	Wood	0.07	−3.57	0.60	0.60	ANU-	11984	6950 ± 180	7950	7610
SMU-4 −40 cm A hp	−3.90	MHWS	Wood	0	−5.05	0.60	0.05	ANUA-	26404	7359 ± 193	8360	7970
SMU-9 +90 cm A	−5.25	MSL	Wood	0	−5.25	0.60	0.60	ANU-	11991	7430 ± 80	8350	8170
SMU-9 +90 cm B	−5.25	MSL	Wood	0	−5.25	0.60	0.60	ANU-	11977	7270 ± 220	8340	7860
SMU-8 +100*	−5.50	MSL	Shell (2)	0.1	−5.45	0.60	0.60	GU-	11246	7590 ± 55	8310	8140
SMU-8 +100 cm*	−5.50	MSL	Wood	0.1	−5.45	0.60	0.60	ANU-	11986	7640 ± 190	8640	8180
SMU-9 +30 cm	−5.65	HAT to MHWS	Wood	0	−7.35	0.60	0.60	ANU-	11992	7640 ± 80	8540	8360
SMU-9 +40 cm	−5.75	HAT to MHWS	Wood	0	−7.45	0.60	0.60	ANU-	11993	7350 ± 100	8330	8020
SMU-8 +10 cm A	−6.40	HAT to MHWS	Wood	0	−8.10	0.60	0.60	ANU-	11980	7660 ± 130	8600	8330
SMU-8 +10 cm B	−6.40	HAT to MHWS	Wood	0	−8.10	0.60	0.60	ANU-	11990	7820 ± 90	8770	8450
MAR-5 +75 cm	−6.97	MSL	Wood	0.28	−6.83	0.62	0.62	ANU-	11841	7530 ± 80	8400	8200

(*continued on next page*)

Table 3 (*continued*)

Sample	Elevation (m)	Indicates	Material	Decompaction (m)	Inferred msl (m)	Error+ (m)	Error− (m)	Prefix	Lab No.	^{14}C age (years BP)/ error (years)	Lower (1σ) (cal BP)	Upper (1σ) (cal BP)
MAR-3A −145 cm	−6.98	MSL	Wood	0.28	−6.84	0.62	0.62	ANU-	11843	7740 ± 100	8610	8400
MAR-4 −205 cm	−7.05	MSL	Wood	0.28	−6.91	0.62	0.62	ANU-	11839	7340 ± 110	8330	8010
MAR-5 +40 cm	−7.42	MHWS	Wood	0	−8.57	0.60	0.05	ANU-	11840	7650 ± 100	8590	8350
MAR-3 −195 cm	−7.48	MHWS	Wood	0	−8.63	0.60	0.05	ANU-	11842	7800 ± 90	8700	8420
STA-1 −10 cm A	−9.02	MSL	Wood	0.38	−8.83	0.63	0.63	ANU-	11996	7910 ± 100	8990	8600
STA-1 −10 cm B	−9.02	MSL	Wood	0.38	−8.83	0.63	0.63	ANU-	11976	7920 ± 80	8980	8610
STA-1 −30 cm B hp	−9.22	HAT to MHWS	Wood	0.15	−10.85	0.60	0.60	ANUA-	26330	7708 ± 192	8950	8200
GEY PS16 bot-15	−14.63	MSL	Wood	0	−14.63	0.60	0.05	ANUA-	25711	8253 ± 243	9550	8750
GEY PS16 76 cm*	−14.64	MSL	Shell	0	−14.64	0.60	0.05	GU-	11252	8050 ± 50	9000	8840
GEY PS16 80 cm*	−14.69	MSL	Wood	0	−14.69	0.60	0.05	GU-	11251	7970 ± 50	8990	8740
GEY PS17 19 cm	−15.09	HAT	Root	0	−17.25	0.60	0.05	ANUA-	25710	8405 ± 246	9700	9000
Hesp et al. (1998)	0.55	MLW or below	Coral (1)	0	1.35	0.4	0.4	WK-	3428	6420 ± 60	7030	6790
Hesp et al. (1998)	0.43	MLW or below	Coral (1)	0	1.23	0.4	0.4	WK-	3429	6270 ± 60	6860	6640
Hesp et al. (1998)	0.25	MLW or below	Coral (1)	0	1.05	0.4	0.4	WK-	3431	6510 ± 60	7160	6930
Hesp et al. (1998)	0.01	MLW or below	Coral (1)	0	0.81	0.4	0.4	WK-	3430	6490 ± 60	7150	6910
Hesp et al. (1998)	−9.59	"Intertidal"	Shell (2)	0	−9.59	1.15	1.15	BETA-	78261	7690 ± 50	8610	8410
Hesp et al. (1998)	−10.40	"Intertidal"	Wood	0	−10.4	1.15	1.15	BETA-	78262	7790 ± 60	8630	8450

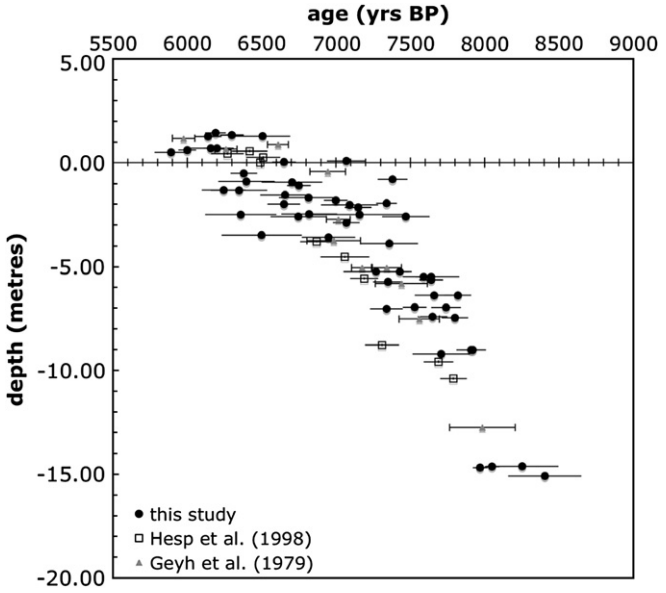

Fig. 3. Radiocarbon age of samples (years BP ±1σ) plotted against sample elevation for all samples from this study and previous studies in the area.

dated from below this depth. The simple sample elevation − uncalibrated radiocarbon age-depth relationship for samples from this study are in agreement with results from earlier studies from Singapore (Hesp et al., 1998) and the nearby Straits of Mallacca (Geyh et al., 1979). More detailed comparison between results from this study and those from the earlier studies, with the exception of the results for coral samples and close-to-basal sample wood/mollusc samples presented by Hesp et al. (1998), is not possible due either to a lack of information on the relationship between dated samples and mean sea-level or to large uncertainties in the amount of compaction undergone by the sedimentary column beneath dated samples. Discussion in the following section is therefore limited to results from this study, but includes those results from Hesp et al. (1998) for which a sufficiently precise link between a sample and mean sea-level at the time of its deposition can be established.

Fig. 4 shows the relationship between calibrated radiocarbon age and the inferred position of mean sea level at the time of sample deposition for those samples where this relationship can be reliably established. The data show less dispersion than in Fig. 3 and suggest the mean sea-level rose from around −17 m at 9350 cal BP at a relatively constant rate up to ∼ −3 m at ∼8000 cal BP at which point there appears to be an inflection, with sea level remaining between −2 and −4 m for a period of several hundred years centred on ∼7700 cal BP. Thereafter MSL again rose to around +1.5 m (or higher) by ∼7000 cal BP.

5. Discussion

5.1. Interpretation of the sea-level curve

Fig. 4 shows evidence of an inflection in the rate of sea-level rise centred on −2 to −4 m, but the interpretation of

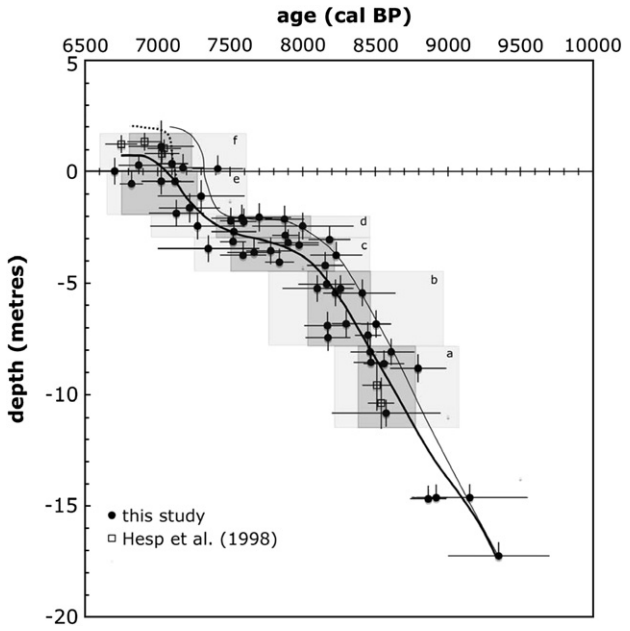

Fig. 4. Calendar age (cal BP ±1σ range) of samples plotted against inferred mean sea-level at the time of sample deposition, with uncertainties in the inferred elevation assigned as described in the text. Boxes a–f delineate sample groups for the purposes of calculating the probability density distributions shown in Fig. 5. Darker shading indicates 1σ interval and lighter shading indicates 2σ interval defined by the PDDs shown in Fig. 5. Dark line is a 6th order polynomial best fit to the data, and dotted line recognizes that any sea level curve, including this line of best fit is constrained to pass above the coral data of Hesp et al. (1998). Thin line delineates a possible trajectory of sea-level rise based on the assumption that the oldest dates at any depth are the most likely to be correct (see text).

this feature is hampered by both the dispersion present in the sample set in the relationship between calendar age and inferred MSL, and also by the comparatively large errors associated with some radiocarbon dates. In order to determine whether the inflection is 'real', the data was broken into sets of seven to eleven samples within depth ranges chosen to isolate sections of the curve before, during and after the apparent inflection. Probability density distributions were calculated for each of these populations using OxCal and the 1σ and 2σ bounds on the calendar age of the populations calculated (Fig. 5). Note that the errors associated with individual radiocarbon dates range widely, but as the range of errors is evenly distributed between sample populations, this should not unduly bias the interpretation.

The PDDs for the lowest elevation groups (a) and (b) are narrow, within a 1σ range of 380 and 440 years respectively, despite being spread over a total vertical interval of 5.4 m. Likewise, the distributions for the highest elevation groups (e) and (f) are within a 1σ range of 500 and 430 years respectively, with samples from these groups spread over a total of 3.1 m. In contrast, the PDDs for the middle groups (c) and (d) are spread over a 1σ range of 700 and 660 years respectively, despite these populations being confined to the narrowest vertical interval of 1.97 m.

Simple linear regression of the data in Fig. 4 indicates that on average sea-level rose 1m every ~150 years. If this rate

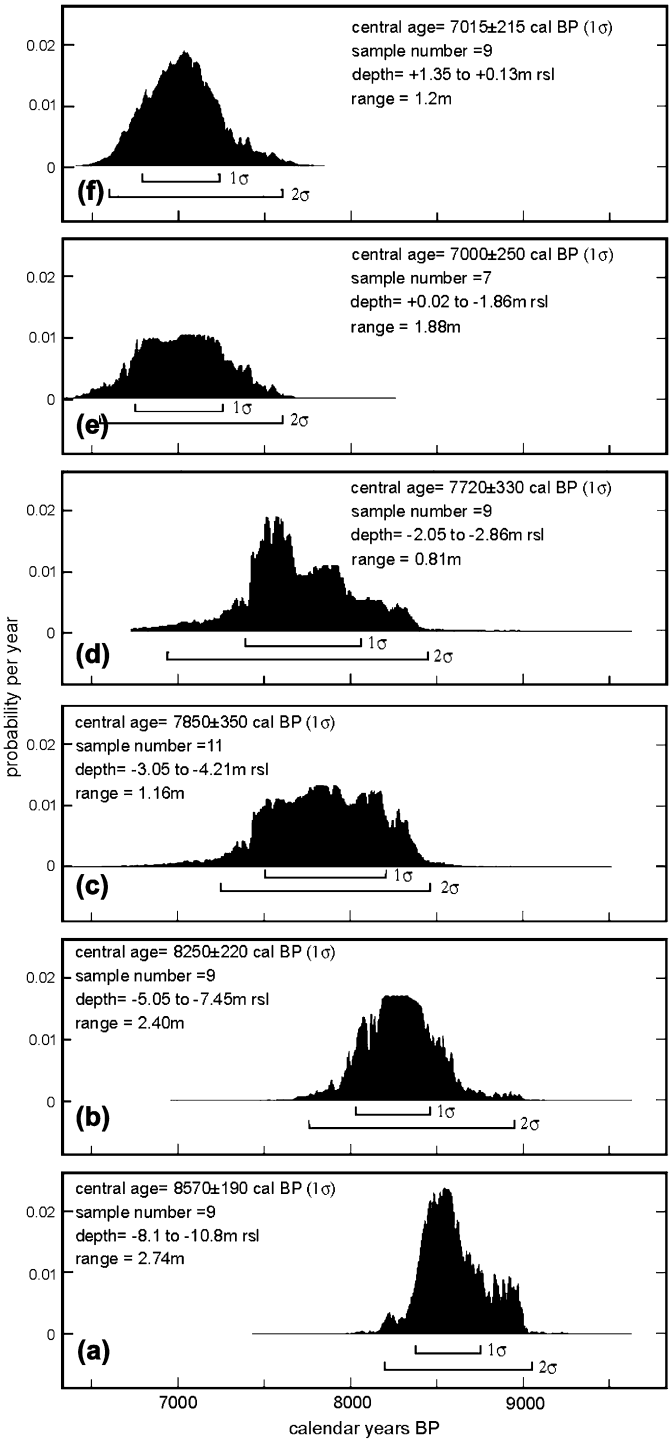

Fig. 5. Probability density distributions and both 1σ and 2σ ranges for samples in groups a-f identified on Fig. 4, along with depth range spanned by the samples in each group.

pertained throughout the period covered in Fig. 4, MSL would have taken 540 years to traverse the vertical interval covered by groups (a) and (b), 200 years to traverse intervals (c) and (d) and 300 years to traverse intervals (e) and (f). Comparison of these figures with the calculated PDDs suggests that while a large portion of the dispersion evident in the upper (e, f) and lower (a, b) groups can be accommodated by the fact that it

took time for sea-level to traverse these intervals, sea-level spent considerably longer within the elevation range of groups (c) and (d) than can be accommodated by the assumption of a constant rate of sea-level rise. There is no reason to believe that any other factors should have led to an increase in the degree of dispersion in groups (c) and (d) relative to groups above and below, and hence the implication is that the rate of sea-level rise slowed, or even stopped over the interval represented by groups (c) and (d).

As there is no hinterland that could supply anomalously old remobilised woody debris (Stanley, 2001) and organic material decays rapidly in tropical environments, it is unlikely that any samples are significantly older than the age of the sediments in which they were deposited. On the other hand, two factors may have resulted in anomalously young ages compared with other samples of equivalent inferred MSL.

First, tidal channels are a common feature of mangrove environments and these can migrate laterally, eroding previously deposited sediments with subsequent infilling by younger sediments at a later time. Thus, it is possible that a sample obtained for dating from a contact assumed to be a sea-level index point, may actually have been deposited at a later time. This could have affected any of the samples at any elevation, and hence the younger dates at a given elevation are more likely to be incorrectly associated with MSL than the older dates at a given elevation.

Second, sea-level fall since the mid Holocene highstand in Singapore has exposed samples from the uppermost elevations (groups e and f) above sea-level within a few metres of the current vegetated ground surface, raising the possibility that some samples may be biased to younger ages by recent contamination. Indeed, one 'wood' sample from 1.3 m above modern sea-level and about 2 m below the pre-excavation ground surface at Kim Chuan Depot returned a radiocarbon activity indicating it was a modern root (KCD7 + 70 cm; ANUA-11995; 102.6 ± 2.1 pMC) Fine networks of rootlets commonly penetrate decayed wood in the deposits sampled for this study and while such material was avoided, the possibility of some contamination from recent rootlet-derived carbon cannot be excluded for samples close to the modern ground surface. This is only a potential issue at elevations within 2–3 m of the modern ground surface due to the large difference in age (~7000 years) between material deposited in the mid Holocene and modern vegetation. This may, for example, explain the comparatively large dispersion in age between samples at ~0 m on Fig. 4 and suggests the older dates are more likely to be correct than the younger dates in this case.

Considering the above, the eighteen dates clustered between −2 and −4 m in Fig. 4 are here interpreted as indicating that MSL remained relatively constant, or rose only slowly for a period of several hundred years centred on ~7700 cal BP. The actual period of slowdown or stillstand is difficult to determine, but may have been as short as from 7800 to 7500 cal BP. Given that there has not been wide recognition of this inflection in global sea-level records, a comparatively short duration for this event is more likely, if it did occur. A sixth order polynomial ($r^2 = 0.92$) provides one possible trajectory for sea-level rise and does delineate the inferred period of slow or no sea-level rise (thick line, Fig. 4). In the uppermost part of this regression, the coral data of Hesp et al. (1998) provides a solid constraint on minimum MSL at around 7000 cal BP, indicating that the post-slowdown rise in MSL was larger than suggested by simple regression of the data, and appears to have amounted to 4–5 m in total (shown by the dotted extension to the thick line on Fig. 4).

Making the assumption, based on the discussion above, that the oldest dates at any depth are the more reliable does not change this overall conclusion, but would make the inflection more pronounced, with the inferred period of sea-level slowdown and subsequent period of sea-level rise occurring slightly earlier (thin line on Fig. 4). Ongoing hydro-isostatic subsidence as a result of the considerable water loading of the Sunda shelf throughout this time period would serve to partly mask a sea-level slowdown, which hence may have been more dramatic than suggested on Fig. 4.

5.2. Comparison with data from other studies

If the interpretation above is correct, the slowdown in, or cessation of, sea-level rise for a few hundred years, centred on ~7700 cal BP should be a global phenomenon, yet is not widely reported. There are several reasons why this might be the case. Studies based on intertidal sea-level indicators are often based on only a few dates, particularly in the time range of interest here, and where comparatively high-resolution studies have been undertaken these are often in regions close to former ice margins where isostatic effects are particularly marked, where tidal ranges are large and variable both in time and space, and the effects of compaction are potentially severe (Allen, 2000; Shennan et al., 2000; Shennan and Horton, 2002). Corals have also provided detailed information on past sea-level, but given that the sea-level slowdown inferred here followed an extended period of rapid rise, including the potentially very rapid rise associated with the catastrophic draining of lakes dammed by the Laurentide ice sheet (Clark et al., 2001; Teller et al., 2002), corals may have had sufficient accommodation space to have grown upwards continuously throughout a comparatively short slowdown in the pace of sea-level rise (e.g. Camoin et al., 2004). Resolution in sea-level records in general remains a problem, exemplified by the fact that the existence of the considerably larger MWP-1B continues to be debated (Okuno and Nakada, 1999; Shennan, 1999).

Even with the high sample density achieved in this study, in a location where isostatic, tectonic, compaction, tidal and storm effects are minimized, where there is no source of ^{14}C depleted groundwater (Lambeck et al., 2004) or of old woody debris remobilised from lacustrine sediments (Stanley, 2001) and the samples were collected over a small area with excellent local survey control on elevation, the existence of the sea-level anomaly inferred above cannot be unequivocally demonstrated. Other evidence that may support the

conclusions of this study comes either from studies that have inferred either 'stepped' sea-level rise during the early mid-Holocene.

Several authors have recently suggested that there have been dramatic changes in the rate of post-glacial eustatic sea-level rise (other than MWP-1 and MWP-2) based on delta and shallow marine stratigraphy, although chronological control on the timing of these variations is generally poor. Detailed mapping of the internal structure of the Yellow River delta and its sub-marine Holocene equivalents has led Liu et al. (2004) to conclude that post-glacial sea-level rise was step-like, with short periods of rapid rise separated by longer periods of slow rise. Of particular significance to the current study is that a final period of rapid rise (termed MWP-1D by Liu et al., 2004) following a period of slow rise, is considered to have been complete by about ~7000 cal BP. Fernández-Salas et al. (2003) have also identified progradation/aggradation cycles in shallow prodelta sediments off southern Spain which they interpret as resulting from changes in eustatic sea-level, including an inferred stillstand in relative sea-level between ~7000 and 8000 cal BP.

The chronological control on the timing of the events identified in the above studies is not good, but they do provide evidence that sea-level rise in the early to mid-Holocene was not monotonic, and other studies are accompanied by more detailed chronologies. MWP-2, originally proposed by Blanchon and Shaw (1995), was inferred to have occurred 'catastrophically' around 7500–7600 cal ka BP and been complete by 7400 cal BP, with the jump in sea-level 'drowning' coral reefs at many localities in the Caribbean. The reality of MWP-2 has been called into question by other coral reef chronologies that have identified corals that appear to have grown throughout the interval proposed for MWP-2 (e.g. Toscano and Lundberg, 1998), however Blanchon et al. (2002) have contended that the corals dated by Toscano and Lundberg (1998) were actually part of a relict boulder ridge and hence could not be used as a constraint of sea-level. The timing of 'classical' MWP-2 is possibly earlier and more rapid than the apparent resumption of sea-level rise suggested in this study, although: (1) as discussed above, the older dates in this study may be more reliable, particularly at higher elevations; and (2) several of the corals dated by Blanchon and Shaw (1995) and Blanchon et al. (2002) did not actually begin to regrow at their new, higher elevation until ~7100 cal BP. The magnitude of the rise inferred here (4–5 m) is similar to the 6.5 ± 2.5 m rise inferred by Blanchon and Shaw (1995).

A study by Engels et al. (2004) has provided further information on reef development on Molokai over the time interval of interest here. The radiocarbon data cannot be used to infer a sea-level history, but does suggest a gap in reef development between ~8000 and ~6900 cal BP (calibrated using an average ΔR for Hawaiian waters of -19 ± 29 years; Intcal marine dataset). This data could be interpreted in the same way as the data of Blanchon et al. (2002), with a period of erosion accompanying a sea-level stillstand shortly after 8000 cal BP, with renewed coral growth further upslope and inshore after a significant (but unquantifiable) rise in sea-level that was complete by 6900 cal BP. Several other studies have suggested rapid periods of sea-level rise either during (Anderson et al., 2001; Bratton et al., 2003) or shortly after (Scott et al., 1995) 7000–8000 cal BP, although none of the results in these studies are amenable to a unique interpretation.

All of the major sea-level curves based on the dating of corals (Huon, Barbados and Tahiti) are characterized by very sparse data between 8000 and 7500 cal BP compared with younger and older intervals (see summaries by Lambeck and Chappell, 2001 and Lambeck et al., 2002a,b), a feature suggestive of a period of little accommodation space to support upward coral growth at this time. The minimum sea-level curve for the Great Barrier Reef presented by Lambeck (2002) could be interpreted as indicating an inflection at around 7500–8000 cal BP, while the eustatic sea-level curve for Italy of Lambeck et al. (2004), is also (but not uniquely) consistent with a slowdown in sea-level rise after ~8000 cal BP, with renewed sea-level rise beginning shortly before ~7000 cal BP. The single coral sequence that Camoin et al. (2004) consider to have closely tracked sea-level throughout the Holocene (Mayotte, PMI-7) indicates a sharp deceleration in the rate of sea-level rise from 0.57 cm/years prior to 8000 cal BP to 0.1 cm/years from 8000 cal BP until the present. Unfortunately the sea-level curve post-dating 8000 cal BP is only constrained by three dates, and hence, while the data do suggest a slowdown at ~8000 cal BP they could not resolve an inflection after 8000 cal BP of the magnitude inferred in this paper.

There is other geomorphic and stratigraphic evidence that supports the inference of a period of slow or no sea-level rise shortly after ~8000 cal BP. Blanchon et al. (2002) provided evidence for a relict submerged sea-cliff at −19 m around Grand Cayman Island with a pronounced inter-tidal notch developed in the sea-cliff for several kilometres on the western side of the island. The notch in particular suggests that a stable shoreline was established at this level for an extended period of time, and dating of corals from the relict reef flat in front of the notch and younger corals subsequently established on top of the sea-cliff indicate that the notch was developed between 8100 and 7600 cal BP. Similarly, Larcombe and Carter (1998) present evidence for an extensive submerged transgressive beach deposit in Cleveland Bay (Queensland, Australia) considered to represent a shoreline developed during period of relative sea-level stability between ~8200 cal BP and ~7500 cal BP, after which the shoreline was rapidly transgressed.

Tanabe et al. (2003) studied the stratigraphy of the Red River delta and determined that prior to ~7100 cal BP, the delta built up above the sea-level of the time, and soils developed on the exposed delta sediments. At, or shortly before, ~7100 cal BP, the delta was rapidly transgressed leading to shelly marine sediment being deposited above the earlier sub-aerially exposed sediments and separated from them by an erosive 'maximum flooding surface'. These data are consistent with a sub-aerial delta being built up under conditions of relative sea-level stability, but then being rapidly transgressed as sea-level rise was renewed.

Circumstantial support for the period of relative sea-level stability suggested here comes from a compilation of data on the timing of the initiation of the major deltas of the world (Stanley and Warne, 1994). A modal peak in the timing of delta initiation occurred between ~8200 and 7800 cal BP, at which time approximately one third of the major deltas in the sample set began to develop. The slowdown in sea-level rise inferred above, occurring at or shortly after this time, may have enabled the deposition of a 'foundation' of sediment under conditions of relatively stable sea-level that subsequently enabled deltas to keep up with continued sea-level rise later in the Holocene. Only 20% of the deltas surveyed by Stanley and Warne (1994) have basal dates indicating they began to develop after this time, and Stanley and Warne (1994) considered that most of these younger ages may not actually represent the earliest phase of delta development, with the comparatively young dates relating to samples collected from the more landward portions of the deltas.

5.3. An explanation for a sea-level inflection centred on 7500 cal BP

The reason for the inferred slowdown in the rate of sea-level rise may be quite straightforward, as melting of the largest continental ice-cap of the LGM, the Laurentide ice-cap, is thought to have been complete by ~7800 cal BP (Clark et al., 2001), with meltwater contributions from Eurasian icecaps and Greenland having ceased prior to this time (Peltier, 2002). In the absence of additional meltwater input from the Antarctic ice-cap, this should have resulted in eustatic sea-level stabilizing at this time and in some ways it would be remarkable if the cessation of melting in the northern hemisphere was synchronously and seamlessly taken up by an increase meltwater input from other sources.

The timing and magnitude of meltwater input from Antarctica is currently poorly constrained, with estimates ranging 37 m metres of equivalent sea-level beginning shortly after the LGM and finishing around 7000 cal BP to as little as 11 m beginning around 12,500 cal BP and completed by around 7000 cal BP (e.g. Nakada et al., 2000). In addition, several researchers have concluded that 3–5 metres of equivalent eustatic sea-level rise are attributable to meltwater input from Antarctica that continued into the middle and later Holocene (Nakada and Lambeck, 1988; Nakada et al., 2000; Lambeck et al., 2004).

Melting of Antarctic ice during most of the deglacial period is thought to have been driven by melting in the northern hemisphere through the destabilizing effect of increasing sea-level on the Antarctic ice margin (Nakada et al., 2000). The West Antarctic Ice Sheet in particular is thought to be relatively unstable, though whether it responds rapidly to changing sea-level or more slowly over a period of centuries is currently unclear (e.g. Oppenheimer, 1998a). While sea-level rise during early deglacial times may provide a mechanism for coupling melting between the hemispheres, this link is less clear for the Holocene. This is because the predictions for relative sea-level, as differentially experienced around the margins of Antarctica, are highly dependent on the amount of isostatic uplift accompanying melting of the Antarctic ice cap itself. Thus different parts of the East and West Antarctic ice margins may have experienced either relative sea-level rise or fall at varying times during the early Holocene, depending on the amount, timing and location of melting (Nakada et al., 2000).

The likely role of relative sea-level changes in triggering further Antarctic melting cannot be assessed in detail due to the paucity of data, however, Conway et al. (1999) demonstrate that while the grounding line of the West Antarctic Ice Sheet had retreated only a comparatively short distance from its LGM position by the early Holocene, rapid retreat occurred in the middle Holocene, beginning 7500 cal BP. Likewise, Stone et al. (2003) has presented convincing evidence for significant thinning of at least part of the West Antarctic Ice Sheet throughout the Holocene. Thus, while the rates and timing of Antarctic melting remain poorly constrained, a period of comparatively rapid meltwater input from Antarctica, beginning around 7500 cal BP or shortly thereafter would explain the renewal of sea-level rise suggested here and be consistent with the currently available evidence from Antarctica.

6. Conclusions

The relative sea-level curve developed here for Singapore constrains sea-level rise in the region over 3000 years between ~9500 and 6500 cal BP. As well as delineating a period of comparatively rapid rise prior to 8000 cal BP, the sea-level curve is interpreted as indicating an inflection in the rate of sea-level rise, with a period of slow or no rise centred on ~7700 cal BP followed by a return to more rapid rates of rise after ~7300 cal BP. Dispersion in the data means that this inflection cannot be said to have been unequivocally demonstrated, but is consistent with other evidence of: (1) stable shorelines and delta development at this time; and (2) the cessation of melting of the northern hemisphere ice-sheets before the inferred inflection and the possible renewal of melting of the Antarctic icesheet after the inferred inflection. The timing of the resumption of sea-level rise is poorly constrained to between ~7400 and ~7200 cal BP, which is slightly later and probably less rapid than the sea-level rise considered to be associated with MWP-2 (7500 to 7600 cal BP; Blanchon and Shaw, 1995; Blanchon et al., 2002) but of similar magnitude (3–5 m).

The trajectory for eustatic sea-level rise proposed above has significant implications for the possible timings and motivations of human migration following the LGM, as human dispersal is thought to have long been associated with coastlines (e.g. Stringer, 2000). Low-lying and resource-rich deltas (Budel, 1964), are thought to have attracted human colonization soon after their initiation and the development of deltas may have encouraged a trend to permanent settlement and the development of agriculture from around ~8000 cal BP (Stanley and Warne, 1997). Rising sea-level throughout deglaciation must have led to the continual movement of populations to higher ground, but would not prompt discrete dispersal 'events'. The

period of comparatively stable sea-level proposed above would promote the colonization of low-lying areas, while the subsequent return to comparatively rapidly rising sea-level may have prompted widespread dispersal, and particularly maritime dispersal, focused into a narrow time interval. This type of human dispersal 'event' has been proposed for the early Holocene by Oppenheimer (1998b) and similar dispersal events could have accompanied other inferred periods of rapid sea-level rise following the LGM.

Acknowledgments

This research was supported by Academic Research Fund grants RP19/01MB and RP20/02MB to MIB, CHC and TST. We wish to acknowledge the support of the following in very generously facilitating access to the sites sampled for this study: Howard Rosser, Nick Osborne, Joshua Ong, Prebarahan Nadarajah, Chiam Sing Lih, Michael Eng, Lim Han Chong, Richard Page and Hong Zhu (Land Transport Authority, Singapore); Gary Png, Anthony Lim and Kato Tetsuya (Singapore Management University); Dennis Khoo and Roger Kung (National Library construction site); John Miksic (National University of Singapore), Ng Ching Huei and Cheryl-Ann Low (National Heritage Board); Joseph Lai (Sungei Buloh Wetland Reserve).

References

Aksu, A.E., Hiscott, R.N., Yasar, D., Isler, F.I., Marsh, S., 2002. Seismic stratigraphy of Late Quaternary deposits from the southwestern Black Sea shelf: evidence for non-catastrophic variations in sea-level during the last ~10 000 yr. Marine Geology 190, 61–94.

Allen, J.R.L., 2000. Holocene coastal lowlands: autocompaction and the uncertain ground. In: Pye, K., Allen, J.R.L. (Eds.), Coastal and Estuarine Environments: Sedimentology, Geomorphology and Geoarchaeology. Geological Society of London, Special Publication 175, 239–252.

Alley, R.B., Mayewski, P.A., Sower, T., Stuiver, M., Taylor, K.C., Clark, P.U., 1997. Holocene climatic instability: a prominent, widespread event 8200 years ago. Geology 25, 483–486.

Anderson, J., Rodriguez, A., Fletcher, C., Fitzgerald, D., 2001. Researchers focus attention on coastal response to climate change. Eos Trans Am Geophys Union 82 (513), 519–520.

Ballard, R.D., Coleman, D.F., Rosenberg, G.D., 2000. Further evidence of abrupt Holocene drowning of the Black Sea shelf. Marine Geology 170, 253–261.

Bard, E., Hamelin, B., Arnold, M., Montaggioni, L.F., Cabioch, G., Faure, G., Rougerie, F., 1996. Deglacial sea-level record from Tahiti corals and the timing of global meltwater discharge. Nature 382, 241–244.

Bird, M.I., Pang, W.C., Lambeck, K. The age and origin of the Straits of Singapore. Palaeogeography, Palaeoclimatology, Palaeoecology, in press.

Bird, M.I., Tan, T.S., The, T.S., Chang, C.H., Shirlaw, N., 2003. Age and Origin of the Quaternary Sediments of Singapore. Proceedings of the 'Underground 2003' Conference, Singapore, September 2003.

Bird, M.I., Chua, S., Fifield, L.K., Teh, T.S., Lai, J., 2004a. Evolution of the Sungei Buloh – Kranji Mangrove coast, Singapore. Applied Geography 24, 181–198.

Bird, M.I., Chua, S., Fifield, L.K., Goh, B., 2004b. Calculating sediment compaction from radiocarbon dating of intertidal sediments. Radiocarbon 46, 421–432.

Blanchon, P., Shaw, J., 1995. Reef drowning during the last deglaciation: evidence for catastrophic sea-level rise and ice-sheet collapse. Geology 23, 4–8.

Blanchon, P., Jones, C., Ford, D.C., 2002. Discovery of a submerged relic reef and shoreline off Grand Cayman: further support for an early Holocene jump in sea level. Sedimentary Geology 147, 253–270.

Bratton, J.F., Colman, S.M., Robert Thieler, E.R., Seal II, R.R., 2003. Birth of the modern Chesapeake Bay estuary between 7.4 and 8.2 ka and implications for global sea-level rise. Geo-Marine Letters 22, 188–197.

Bronk Ramsey, C., 2001. Development of the Radiocarbon Program OxCal. Radiocarbon 43, 355–363.

Budel, J., 1964. Deltas – a basis of culture and civilization. Scientific Problems of the Humid Tropical Zone Deltas and Their Implications.. In: Proceedings of the Dacca Symposium, Dacca, 24th February to 2nd March, 1964 UNESCO, pp. 295–300.

Camoin, G., Montaggioni, L., Braithwaite, C., 2004. Late glacial to post glacial sea levels in the Western Indian Ocean. Marine Geology 206, 119–146.

Clark, P.U., Mix, A.C., 2002. Ice sheets and sea level of the Last Glacial Maximum. Quaternary Science Reviews 21, 1–7.

Clark, P.U., Marshall, S., Clarke, G., Licciardi, J., Teller, J., 2001. Freshwater forcing of abrupt climate change during the last glaciation. Science 293, 283–287.

Conway, H., Hall, B.L., Denton, G.H., Gades, A.M., Waddington, E.D., 1999. Past and future grounding-line Retreat of the West Antarctic. Ice sheet. Science 286, 280–283.

Engels, M.S., Fletcher III, C.H., Field, M.E., Storlazzi, C.D., Grossman, E.E., Rooney, J.J.B., Conger, C.L., Glenn, C., 2004. Holocene reef accretion: southwest Molokai, Hawaii, U.S.A. Journal of Sedimentary Research 74, 255–269.

Fairbanks, R.G., 1989. A 17,000-year glacio-eustatic sea level record: influence of glacial melting rates on the Younger Dryas event and deep-ocean circulation. Nature 342, 639–642.

Fernández-Salas, L.M., Lobo, F.J., Hernández-Molina, F.J., Somoza, L., Rodero, J., Díaz del Río, V., Maldonado, A., 2003. High-resolution architecture of late Holocene highstand prodeltaic deposits from southern Spain: the imprint of high-frequency climatic and relative sea-level changes. Continental Shelf Research 3, 1037–1237.

Geyh, M.A., Kudrass, H.R., Streif, H., 1979. Sea-level changes during the late Pleistocene and Holocene in the Straits of Malacca. Nature 278, 441–443.

Gupta, A., Rahman, A., Wong, P.P., Pitts, J., 1987. The Old Alluvium and the extinct drainage system to the South China Sea. Earth Surface Processes and Landforms 12, 259–275.

Hanebuth, T., Stattegger, K., Grootes, P.M., 2000. Rapid flooding of the Sunda Shelf: a late Glacial sea-level record. Science 288, 1033–1035.

Hesp, P.A., Chang, C.H., Hilton, M., Ming, C.L., Turner, I.M., 1998. A first tentative Holocene sea-level curve for Singapore. Journal of Coastal Research 14, 308–314.

Hilton, M.J., Ming, C.L., 1999. sediment facies of a low energy, meso-tidal fringing reef, Singapore. Singapore Journal of Tropical Geography 20, 111–130.

Lambeck, K., 2002. Sea-Level change from mid-Holocene to recent time: an Australian example with global implications. In: Mitrovica, J.X., Vermeersen, B. (Eds.), Glacial Isostatic Adjustment and the Earth System. American Geophysical Union, Washington, DC, pp. 33–50.

Lambeck, K., Chappell, J., 2001. Sea-level change through the last glacial cycle. Science 292, 679–686.

Lambeck, K., Yokoyama, Y., Purcell, T., 2002a. Into and out of the Last Glacial Maximum: sea-level change during oxygen-isotope stages 3 and 2. Quaternary Science Reviews 21, 343–360.

Lambeck, K., Esat, T.M., Potter, E., 2002b. Links between climate and sea levels for the past three million years. Nature 419, 199–206.

Lambeck, K., Antonioli, F., Anthony Purcell, A., Silenzi, S., 2004. Sea-level change along the Italian coast for the past 10,000 yr. Quaternary Science Reviews 23, 1567–1598.

Larcombe, P., Carter, R.M., 1998. Sequence architecture during the Holocene transgression: an example from the Great Barrier Reef shelf, Australia. Sedimentary Geology 117, 97–121.

Liu, J.P., Milliman, J.D., Gao, S., Peng, C., 2004. Holocene development of the Yeoow River's sub-aqueous delta, North Yellow Sea. Marine Geology 209, 45–67.

Nakada, M., Lambeck, K., 1988. The melting history of the Late Pleistocene Antarctic Ice Sheet. Nature 333, 36–40.

Nakada, M., Kimura, R., Okuno, J., Moriwaki, K., Miura, H., Maemoku, H., 2000. Late Pleistocene and Holocene melting history of the Antarctic ice sheet derived from sea-level variations. Marine Geology 167, 85–103.

Okuno, J., Nakada, M., 1999. Total volume and temporal variation of meltwater from last interglacial maximum inferred from sea-level observations at Barbados and Tahiti. Palaeogeography, Palaeoclimatology, Palaeoecology 146, 283–293.

Oppenheimer, M., 1998a. Global warming and the stability of the west Antarctic icesheet. Nature 393, 325–331.

Oppenheimer, S., 1998b. Eden in the East: The Drowned Continent of Southeast Asia. Guernsey, Phoenix, 560 pp.

Peltier, W.R., 2002. On eustatic sea level history: Last Glacial Maximum to Holocene. Quaternary Science Reviews 21, 377–396.

Pitts, J., 1983. The Origin, Nature and Extent of Recent Deposits in Singapore. Proceedings International Seminar on Construction Problems in Soft Soils. 1st–3rd December, 1983, Singapore JP1-JP18.

PWD, 1976. Geology of the Republic of Singapore. Public Works Department, 79 pp.

Ryan, W.B.F., Pitman, W.C., Major, C.O., Shimkus, K., Moskalenko, V., Jones, G.A., Dimitrov, P., Goriir, N., Saking, M., Yiice, H., 1997. An abrupt drowning of the Black Sea shelf. Marine Geology 138, 119–126.

Scott, D.B., Gayes, P.T., Collins, E.S., 1995. Mid-Holocene precedent for a future rise in sea-level along the Atlantic coast of North America. Journal of Coastal Research 11, 615–622.

Shennan, I., 1999. Global meltwater discharge and the deglacial sea-level record from northwest Scotland. Journal of Quaternary Science 14, 715–719.

Shennan, I., Horton, B., 2002. Holocene land- and sea-level changes in Great Britain. Journal of Quaternary Science 17, 511–526.

Shennan, I., Lambeck, K., Horton, B., Innes, J., Jerry Lloyd, J., McArthur, J., Purcell, T., Rutherford, M., 2000. Late Devensian and Holocene records of relative sea-level changes in northwest Scotland and their implications for glacio-hydro-isostatic modelling. Quaternary Science Reviews 19, 1103–1135.

Southon, J., Kashgarian, M., Fontugne, M., Metivier, B., Yim, W.W.-S., 2002. Marine reservoir correction for the Indian Ocean and Southeast Asia. Radiocarbon 44, 167–180.

Stanley, D.J., 2001. Dating modern deltas: progress, problems and prognostics. Annual Reviews of Earth and Planetary Sciences 29, 257–294.

Stanley, D.J., Warne, A.G., 1994. Worldwide initiation of Holocene marine deltas by deceleration of sea-level rise. Science 265, 228–231.

Stanley, D.J., Warne, A.G., 1997. Holocene sea-level change and early human utilization of deltas. GSA Today 7, 1–7.

Stone, J.O., Balco, G., Sugden, D.E., Caffee, M.W., Sass III, L.C., Cowdery, S.G., Siddoway, C., 2003. Late Holocene Deglaciation of Marie Byrd Land, West Antarctica. Science 299, 99–102.

Stringer, C., 2000. Coasting out of Africa. Nature 405, 24–27.

Stuiver, M., Reimer, P.J., Braziunas, T.F., 1998. High-precision radiocarbon age calibration for terrestrial and marine samples. Radiocarbon 40, 1127–1151. Available from: http://www.calib.org/.

Tanabe, S., Kazuaki Hori, K., Saito, Y., Haruyama, S., Doanh, L.Q., Sato, Y., Shigenobu Hiraide, S., 2003. Sedimentary facies and radiocarbon dates of the Nam Dinh-1 core from the Song Hong (Red River) delta, Vietnam. Journal of Asian Earth Sciences 21, 503–513.

Teller, J.T., Leverington, D.W., Mann, J.D., 2002. Freshwater outbursts to the oceans from glacial Lake Agassiz and climate change during the last deglaciation. Quaternary Science Reviews 21, 879–887.

Tjia, H.D., 1992. Holocene sea-level changes in the Malay-Thai Peninsula, a tectonically stable environment. Geological Society of Malaysia Bulletin 31, 157–176.

Toscano, M.A., Lundberg, J., 1998. Early Holocene sea-level record from submerged fossil reefs on the southeast Florida margin. Geology 26, 255–258.

Wong, P.P., 1992. Impact of a sea level rise on the coasts of Singapore: preliminary observations. Journal of Southeast Asian Earth Sciences 7, 65–70.